Journal of GeoEngineering, Vol. 11, No. 1, pp. 33-43, April 2016
http://dx.doi.org/10.6310/jog.2016.11(1).4

SIMULATING A CURVE AVERAGE IN A STATIONARY NORMAL RANDOM FIELD USING FOURIER SERIES METHOD

Jianye Ching[1*] and Shang-Ping Sung[2]

ABSTRACT

Spatial averaging along a curve in two dimensions (2D) is of practical interest to geotechnical engineers, because it is the averaged soil shear strength along the critical slip curve that governs the ultimate failure of a 2D spatially variable soil mass. However, techniques that are able to simulate such a "curve average" are not available in the literature, because the random process along a curve is in general non-stationary, even if the 2D random field is stationary. This paper proposes a method of simulating such a curve average in a 2D stationary normal random field for a curve approximated by connecting line segments. This method is also able to calculate the variance reduction factor due to the approximate curve averaging. The proposed method is validated by several 1D problems with analytical solutions. It is shown that the proposed method produces results identical to the 1D analytical solutions. Two geotechnical analysis examples are used to demonstrate the applications of the proposed method.

Key words: Spatial variability, curve averaging, random field, geotechnical engineering, slope stability.

1. INTRODUCTION

Random field models have been adopted to model the spatial variability of geotechnical materials (Vanmarcke 1977). In particular, they have become increasingly popular in the recent decades in modeling the spatial variability of soil/rock shear strength (Asaoka and Grivas 1982; Soulie *et al*. 1990; Fenton and Griffiths 2003; Griffiths and Fenton 2004; Chok *et al*. 2007; Griffiths *et al*. 2010; Nishimura *et al*. 2010; Wang *et al*. 2011; Ching and Liao 2013). It is generally accepted that it is the spatial average of the shear strength that governs the ultimate failure of a geotechnical structure. For instance, the vertical resistance of a friction pile is governed by the average of the spatially variable shear strength along the pile shaft (*e.g.*, Cao *et al*. 2013). In a two-dimensional (2D) slope stability problem, the safety factor of a trial slip curve is governed by the averaged shear strength over the curve (*e.g.*, El-Ramly *et al*. 2002; Cho 2007). Even for a 2D soil column, the mobilized shear strength is governed by the average along the critical failure curve (Ching and Phoon 2013a, 2013b). It is therefore imperative to simulate spatial averages of a 2D random field along curves.

The spatial average of a 2D random field over a prescribed rectangular volume can be simulated using existing methods, including the Local Average Subdivision (LAS) method (Fenton and Vanmarcke 1990) and the Fourier series method (Jha and Ching 2013). However, none of these methods is able to simulate spatial averages along curves in 2D. The above mentioned Fourier series method is able to simulate the spatial average along a single line segment (Jha and Ching 2013), namely a "line average", but this method cannot simulate a "curve average". Methods for simulating curve averages are rare in the literature probably because the random process along a curve is in general non-stationary, even if the 2D random field is stationary. Figure 1(a) demonstrates such a scenario. In this scenario, the 2D random field is stationary with horizontal scale of fluctuation (SOF) δ_x = 100 and vertical SOF δ_z = 2. The curve of interest is the circle shown in the figure. Figure 1(b) shows the random process along the circle. It is clear that the SOF along this circle is not a constant, hence the random process is non-stationary. Analytical methods for simulating the curve average are not available in the literature, although simulating a curve average is an important subject in geotechnical engineering.

On the other hand, geotechnical analysis frequently uses a series of connecting line segments to approximate a curve, *e.g.*, the method of slices in slope stability (*e.g.*, Duncan and Wright 2005). The random process along a straight line segment is guaranteed to be stationary if the 2D random field is stationary. If a curve is approximated by the connecting line segments (Fig. 1(a)), the non-stationary random process along the curve is therefore approximated by a piecewise stationary random process along the line segments (Fig. 1(c)). The spatial average along the curve (curve average) can therefore be approximately represented by the weighted sum of the line averages along these line segments. This requires the *simultaneous* simulations of the line averages. The Fourier series method developed by Jha and Ching (2013) can simulate these line averages *individually*. However, in order to *simultaneously* simulate these line averages, the covariance among these line averages must be properly quantified. Jha and Ching (2013) did not address this aspect. Vanmarcke (1983) derived the analytical expression for the covariance between two line averages in one dimension (1D). However, this formula is not applicable to 2D. El-Ramly *et al*. (2002) adopted the covariance between the midpoints of two line segments as an approximation. Cho (2007) evaluated the covariance between line averages using numerical integration.

Manuscript received November 20, 2015; revised February 17, 2016; accepted February 23, 2016.
[1] Professor (corresponding author), Dept. of Civil Engineering, National Taiwan University, Taipei, Taiwan (e-mail: jyching@gmail. com).
[2] Graduate student, Dept. of Civil Engineering, National Taiwan University, Taipei, Taiwan.

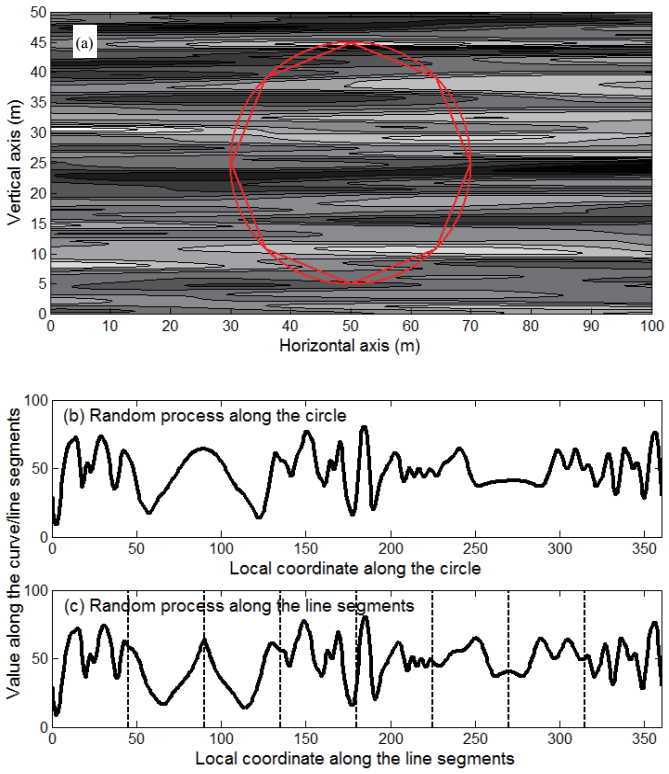

Fig. 1 (a) An anisotropic random field realization; (b) The random process along the circle; (c) The random process along the line segments

The purpose of this paper is to develop a method of approximately simulating curve averages in a 2D stationary normal random field. As mentioned earlier, the curve of interest will be first approximated by a series of connecting line segments. Hence, the curve average can be approximated as the weighted sum of the line averages. The key component of this method is to represent the covariance between any two line averages in 2D using the Fourier series method. With the knowledge of all covariances, it will be clear later that the variance reduction factor for the curve averaging can be computed approximately. Two geotechnical analysis examples of curve averages will be demonstrated in this paper, including the spatial average along a circle and that along an arc of a circle. The MATLAB codes for approximately simulating the curve average and computing the variance reduction factor are available to the readers upon request (please contact the first author).

2. 2D STATIONARY RANDOM FIELDS

Among random field models, stationary (or statistically homogeneous) random fields are widely used due to their simplicity and possibly the only practical version that can be characterized statistically from limited data (Phoon *et al*. 2003). A 2D stationary random field $W(x, z)$ can be defined over a plane with x = horizontal coordinate and z = depth coordinate. This random filed is characterized by three parameters: (a) inherent mean $E(W) = \mu$, (b) inherent variance $Var(W) = \sigma^2$, and (c) auto-correlation function (ACF). The ACF of a stationary random field $W(x,z)$ is defined as the correlation between two locations Δx apart horizontally in the x-direction and Δz apart vertically in the z-direction:

$$\rho(\Delta x, \Delta z) = \rho\left[W(x, z), W(x+\Delta x, z+\Delta z)\right] = \frac{CV\left[W(x, z), W(x+\Delta x, z+\Delta z)\right]}{\sqrt{Var\left[W(x, z)\right]}\cdot\sqrt{Var\left[W(x+\Delta x, z+\Delta z)\right]}} \quad (1)$$

where $Var(.)$ denotes variance; $CV(., .)$ denotes covariance. The hypothesis of stationarity allows ρ to be simplified as a function of Δx and Δz only, rather than the absolute coordinates (x, z) and $(x + \Delta x, z + \Delta z)$ [see left hand side of Eq. (1)]. The most popular ACF is the single exponential (SExp) model:

$$\rho(\Delta x, \Delta z) = \exp\left(-2\,|\Delta x|/\delta_x - 2\,|\Delta z|/\delta_z\right) \quad (2)$$

where δ_x and δ_z are respectively the scales of fluctuation (SOFs) in the x and z directions. Another popular ACF is the squared exponential (QExp) model:

$$\rho(\Delta x, \Delta z) = \exp\left[-\pi\,(\Delta x/\delta_x)^2 - \pi\,(\Delta z/\delta_z)^2\right] \quad (3)$$

It is clear that the correlation decreases as Δx and Δz increase. Because of the manner in which most natural soils are deposited, soil properties are expected to be strongly correlated over a small interval and weakly correlated when measurement points are sufficiently far apart.

2.1 Simulation of Point Process

Jha and Ching (2013) developed the Fourier-series method (FSM) for simulating 2D stationary normal random fields (point process). Consider a 2D stationary normal random field $W(x, z)$ over a simulation domain of size $L_x \times L_z$. This random field can be simulated by

$$W(x, z) = \mu + \mathrm{Re}\left[\sum_{m=-\infty}^{\infty}\sum_{n=-\infty}^{\infty}(a_{mn} + ib_{mn})\exp\left(\frac{i2m\pi x}{L_x} + \frac{i2n\pi z}{L_z}\right)\right] \quad (4)$$

where Re[.] denotes the real part of the enclosed complex number; a_{mn} and b_{mn} are independent zero-mean normal random variables with variance σ_{mn}^2 given by

$$\sigma_{mn}^2 = \begin{cases} \dfrac{\sigma^2}{q_x q_z}\left[\dfrac{1-\exp(-q_x)(-1)^m}{1+m^2\pi^2/q_x^2}\right]\times\left[\dfrac{1-\exp(-q_z)(-1)^n}{1+p^2\pi^2/q_z^2}\right] & \text{for SExp} \\ \dfrac{\sigma^2}{q_x q_z}\exp\left(-\dfrac{\pi m^2}{q_x^2} - \dfrac{\pi n^2}{q_z^2}\right) & \text{for QExp} \end{cases} \quad (5)$$

where $q_x = L_x / \delta_x$ and $q_z = L_z / \delta_z$. Without loss of generality, the following discussions will only focus on $\mu = 0$, because it is always possible to produce a random field with mean = μ by adding a constant μ to a zero-mean random field. For the summation above, it is not necessary to sum up to infinite terms. It suffices to sum to $(\pm m, \pm n)$ satisfying the following thumb-rule equations:

$$\begin{cases} \dfrac{1}{q_x}\left[\dfrac{1-\exp(-q_x)(-1)^m}{1+m^2\pi^2/q_x^2}\right]=10^{-6} \quad \dfrac{1}{q_z}\left[\dfrac{1-\exp(-q_z)(-1)^n}{1+n^2\pi^2/q_z^2}\right]=10^{-6} & \text{for SExp} \\ \dfrac{1}{q_x}\exp\left(-\dfrac{\pi m^2}{q_x^2}\right)=10^{-6} \qquad \dfrac{1}{q_z}\exp\left(-\dfrac{\pi n^2}{q_z^2}\right)=10^{-6} & \text{for QExp} \end{cases} \tag{6}$$

The 10^{-6} rule here is slightly more strict than the 10^{-5} rule proposed in Jha and Ching (2013). Also, to circumvent the potential periodic behavior in FSM, Jha and Ching (2013) proposed a simple solution: the simulation space is extended by taking $L_{xE} = L_x + 4\delta_x$ and $L_{zE} = L_z + 4\delta_z$. The details can be found in Jha and Ching (2013).

2.2 Simulation of the Spatial Average Along a Line Segment

For the spatial average along a line segment in 2D with end points (x_0, z_0) and (x_1, z_1). The line average, denoted by W_S, has the following expression:

$$W_S = \int_0^1 W(x_0 + \Delta x \times s,\ z_0 + \Delta z \times s)\, ds \tag{7}$$

where $\Delta x = x_1 - x_0$; $\Delta z = z_1 - z_0$; $s \in [0, 1]$ is the local coordinate along the line: $s = 0$ corresponds to (x_0, z_0), and $s = 1$ corresponds to (x_1, z_1). The above integral has the following analytical expression (Jha and Ching 2013):

$$\begin{aligned} W_S &= \mathrm{Re}\left\{\sum_{m=-\infty}^{\infty}\sum_{n=-\infty}^{\infty}(a_{mn}+ib_{mn})\int_0^1 \exp\left(\frac{i2m\pi(x_0+\Delta x\times s)}{L_x}+\frac{i2n\pi(z_0+\Delta z\times s)}{L_z}\right)ds\right\} \\ &= \mathrm{Re}\left\{\sum_{m=-\infty}^{\infty}\sum_{n=-\infty}^{\infty}\frac{a_{mn}+ib_{mn}}{i2m\pi\Delta x/L_x+i2n\pi\Delta z/L_z}\exp\left(\frac{i2m\pi x_0}{L_x}+\frac{i2n\pi z_0}{L_z}\right)\left[\exp\left(\frac{i2m\pi\Delta x}{L_x}+\frac{i2n\pi\Delta z}{L_z}\right)-1\right]\right\} \end{aligned} \tag{8}$$

Let us denote the constant $(2m\pi x_0/L_x + 2n\pi z_0/L_z)$ by c_{mn} and denote the constant $(2m\pi\Delta x/L_x + 2n\pi\Delta z/L_z)$ by Δ_{mn}. Note that c_{mn} and Δ_{mn} are deterministic real numbers indexed by (m, n): They are not random. It can be shown that Eq. (8) can be written as

$$W_S = \sum_{m=-\infty}^{\infty}\sum_{n=-\infty}^{\infty}\left(\frac{a_{mn}}{\Delta_{mn}}\left[\sin(c_{mn}+\Delta_{mn})-\sin(c_{mn})\right]+\frac{b_{mn}}{\Delta_{mn}}\left[\cos(c_{mn}+\Delta_{mn})-\cos(c_{mn})\right]\right) \tag{9}$$

Note that the operation "Re[.]" does not exist in Eq. (9). Equation (9) is the basis for the derivations for the "curve average" below. For certain combinations of (m, n), it is possible that $\Delta_{mn} = 0$. For these (m, n) combinations, the term inside the summation sign in Eq. (9) should be replaced (L'Hospital's rule):

$$\frac{a_{mn}}{\Delta_{mn}}\left[\sin(c_{mn}+\Delta_{mn})-\sin(c_{mn})\right]+\frac{b_{mn}}{\Delta_{mn}}\left[\cos(c_{mn}+\Delta_{mn})-\cos(c_{mn})\right]\xrightarrow[\text{replaced by}]{} a_{mn}\cos(c_{mn})-b_{mn}\sin(c_{mn}) \tag{10}$$

3. CURVE AVERAGING FOR 2D STATIONARY NORMAL RANDOM FIELDS

In this study, a curve is approximated by a series of connecting line segments (S_1, S_2, …, S_n) (see Fig. 2). This is compatible to the practice in geotechnical engineering, *e.g.*, the method of slices in slope stability. These line segments must be sufficiently short in order to maintain a satisfactory representation for the curve. Let us denote the line averages over these n line segments by (W_{S1}, W_{S2}, …, W_{Sn}). For a zero-mean normal random field, (W_{S1}, W_{S2}, …, W_{Sn}) are zero-mean multivariate normal with the following covariance matrix:

$$\mathbf{C} = \begin{bmatrix} Var(W_{S1}) & CV(W_{S1},W_{S2}) & \cdots & CV(W_{S1},W_{Sn}) \\ & Var(W_{S2}) & & CV(W_{S2},W_{Sn}) \\ & & \ddots & \vdots \\ SYM. & & & Var(W_{Sn}) \end{bmatrix} = \begin{bmatrix} C_{11} & C_{12} & \cdots & C_{1n} \\ & C_{22} & & C_{2n} \\ & & \ddots & \vdots \\ SYM. & & & C_{nn} \end{bmatrix} \tag{11}$$

Each W_{Si} is zero-mean because we focus on zero-mean random fields. The main difficulty here is the derivation of the analytical expression for the covariance term $CV(W_{Si}, W_{Sj}) = C_{ij}$ in Eq. (11). One exception is the analytical expression derived by Vanmarcke (1983) for the covariance between two line averages in 1D (z coordinate only):

$$C_{ij} = CV(W_{S_i}, W_{S_j}) = \frac{\sigma^2}{2\cdot L_i\cdot L_j}\sum_{k=0}^{3}(-1)^k\cdot D_k^2\cdot\Gamma^2(D_k) \tag{12}$$

where W_{Si} is the line average along a line segment S_i with length = L_i;

$$W_{Si} = \frac{1}{L_i}\int_{z_{0,i}}^{z_{0,i}+L_i} W(\xi)\, d\xi \tag{13}$$

where $z_{0,i}$ is the z-coordinate of the left-hand-side end point of S_i; the definitions of D_0, D_1, D_2, and D_3 are shown in Fig. 3; $\Gamma^2(D)$ is the variance reduction factor for the 1D averaging effect:

$$\Gamma^2(D) = \begin{cases} \left[2D/\delta - 1 + \exp(-2D/\delta)\right] \Big/ (2D^2/\delta^2) & \text{for SExp model} \\ \left[\pi D/\delta \cdot erf(\sqrt{\pi}\times D/\delta) + \exp(-\pi D^2/\delta^2) - 1\right] \Big/ (\pi D^2/\delta^2) & \text{for QExp model} \end{cases} \tag{14}$$

where δ is the SOF; *erf*(.) is the error function. However, Eq. (12) is for two line segments in 1D, and it is not applicable to two line segments in 2D.

For two line segments in 2D, the covariance term C_{ij} can be readily derived based on Eq. (9). Consider two line segments in 2D, *e.g.*, S_i and S_j in Fig. 4.

$$\begin{aligned} C_{ij} &= CV(W_{Si}, W_{Sj}) = E(W_{Si}\cdot W_{Sj}) \\ &= \sum_{m=-\infty}^{\infty}\sum_{n=-\infty}^{\infty}\sum_{p=-\infty}^{\infty}\sum_{q=-\infty}^{\infty} E\left[\begin{array}{l} \left(\dfrac{a_{mn}}{\Delta_{mn,i}}\left[\sin(c_{mn,i}+\Delta_{mn,i}) - \sin(c_{mn,i})\right] + \dfrac{b_{mn}}{\Delta_{mn,i}}\left[\cos(c_{mn,i}+\Delta_{mn,i}) - \cos(c_{mn,i})\right]\right) \\ \times\left(\dfrac{a_{pq}}{\Delta_{pq,j}}\left[\sin(c_{pq,j}+\Delta_{pq,j}) - \sin(c_{pq,j})\right] + \dfrac{b_{pq}}{\Delta_{pq,j}}\left[\cos(c_{pq,j}+\Delta_{pq,j}) - \cos(c_{pq,j})\right]\right) \end{array}\right] \end{aligned} \tag{15}$$

where ($c_{mn,i}$, $\Delta_{mn,i}$) are for the (c, Δ) parameters of the i-th line segment S_i:

$$c_{mn,i} = 2m\pi x_{0,i}/L_x + 2n\pi z_{0,i}/L_z \quad \Delta_{mn,i} = 2m\pi\Delta x_i/L_x + 2n\pi\Delta z_i/L_z \tag{16}$$

where ($x_{0,i}$, $z_{0,i}$) and ($x_{1,i}$, $z_{1,i}$) are the coordinates of the two end points for the i-th line segment; $\Delta x_i = x_{1,i} - x_{0,i}$ and $\Delta z_i = z_{1,i} - z_{0,i}$. The key fact here is that all random variables (a_{mn}, b_{mn}) in Eq. (15) are zero-mean and mutually independent, so

$$E(a_{mn}\, b_{pq}) = 0 \qquad E(a_{mn}\, a_{pq}) = E(b_{mn}\, b_{pq}) = \sigma_{mn}^2\, \delta_{mp}\, \delta_{nq} \qquad \forall m, n, p, q \tag{17}$$

where δ_{mp} is the Dirac delta function (δ_{mp} = 1 only if $m = p$; otherwise it is 0). As a result, Eq. (15) can be simplified into

$$C_{ij} = \sum_{m=-\infty}^{\infty}\sum_{n=-\infty}^{\infty} \frac{\sigma_{mn}^2}{\Delta_{mn,i}\,\Delta_{mn,j}} \left(\begin{array}{l} \left[\sin(c_{mn,i}+\Delta_{mn,i}) - \sin(c_{mn,i})\right]\times\left[\sin(c_{mn,j}+\Delta_{mn,j}) - \sin(c_{mn,j})\right] \\ \quad + \left[\cos(c_{mn,i}+\Delta_{mn,i}) - \cos(c_{mn,i})\right]\times\left[\cos(c_{mn,j}+\Delta_{mn,j}) - \cos(c_{mn,j})\right] \end{array}\right) \tag{18}$$

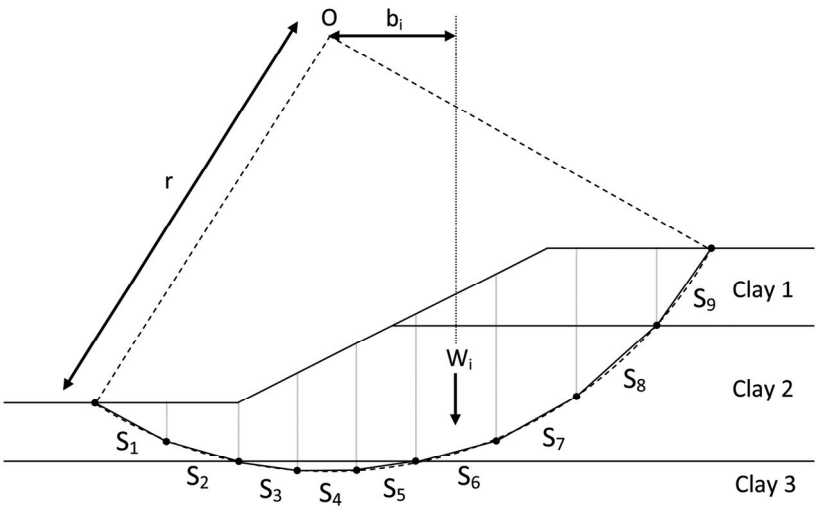

Fig. 2 A potential slip curve divided into 9 line segments. This plot is to the scale (radius r = 30 m).

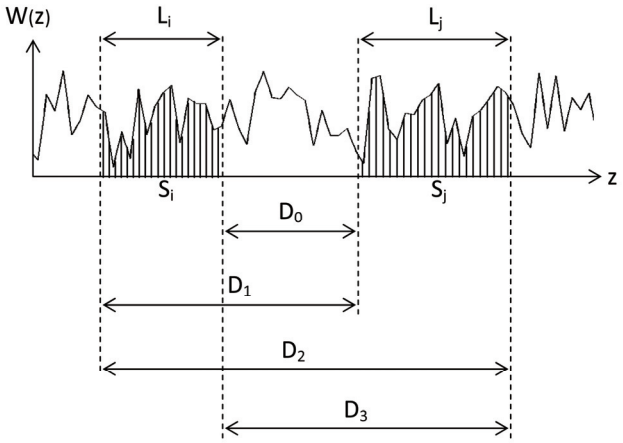

Fig. 3 The definitions of D_0, D_1, D_2, and D_3 (redrawn from Vanmarcke 1983)

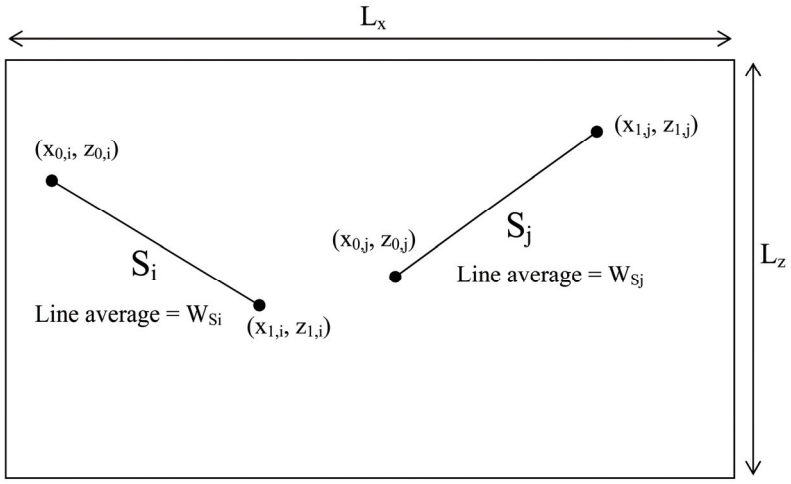

Fig. 4 Two line segments in 2D, S_i and S_j

The formula for σ^2_{mn} can be found in Eq. (5). For certain combinations of (m, n), it is possible that $\Delta_{mn,i} = 0$. For these (m, n) combinations, the term inside the summation sign in Eq. (18) should be replaced:

$$\frac{\sigma^2_{mn}}{\Delta_{mn,i}\,\Delta_{mn,j}}\left(\begin{array}{l}\left[\sin(c_{mn,i}+\Delta_{mn,i})-\sin(c_{mn,i})\right]\times\left[\sin(c_{mn,j}+\Delta_{mn,j})-\sin(c_{mn,j})\right]\\+\left[\cos(c_{mn,i}+\Delta_{mn,i})-\cos(c_{mn,i})\right]\times\left[\cos(c_{mn,j}+\Delta_{mn,j})-\cos(c_{mn,j})\right]\end{array}\right)$$

$$\xrightarrow[\text{replaced by}]{}\frac{\sigma^2_{mn}}{\Delta_{mn,j}}\left(\cos(c_{mn,i})\times\left[\sin(c_{mn,j}+\Delta_{mn,j})-\sin(c_{mn,j})\right]-\sin(c_{mn,i})\times\left[\cos(c_{mn,j}+\Delta_{mn,j})-\cos(c_{mn,j})\right]\right) \tag{19}$$

For the (m, n) combinations with $\Delta_{mn,j} = 0$,

$$\frac{\sigma^2_{mn}}{\Delta_{mn,i}\,\Delta_{mn,j}}\left(\begin{array}{l}\left[\sin(c_{mn,i}+\Delta_{mn,i})-\sin(c_{mn,i})\right]\times\left[\sin(c_{mn,j}+\Delta_{mn,j})-\sin(c_{mn,j})\right]\\+\left[\cos(c_{mn,i}+\Delta_{mn,i})-\cos(c_{mn,i})\right]\times\left[\cos(c_{mn,j}+\Delta_{mn,j})-\cos(c_{mn,j})\right]\end{array}\right)$$

$$\xrightarrow[\text{replaced by}]{}\frac{\sigma^2_{mn}}{\Delta_{mn,i}}\left(\cos(c_{mn,j})\times\left[\sin(c_{mn,i}+\Delta_{mn,i})-\sin(c_{mn,i})\right]-\sin(c_{mn,j})\times\left[\cos(c_{mn,i}+\Delta_{mn,i})-\cos(c_{mn,i})\right]\right) \tag{20}$$

For the (m, n) combinations with $\Delta_{mn,i} = \Delta_{mn,j} = 0$,

$$\frac{\sigma^2_{mn}}{\Delta_{mn,i}\,\Delta_{mn,j}}\left(\begin{array}{l}\left[\sin(c_{mn,i}+\Delta_{mn,i})-\sin(c_{mn,i})\right]\times\left[\sin(c_{mn,j}+\Delta_{mn,j})-\sin(c_{mn,j})\right]\\+\left[\cos(c_{mn,i}+\Delta_{mn,i})-\cos(c_{mn,i})\right]\times\left[\cos(c_{mn,j}+\Delta_{mn,j})-\cos(c_{mn,j})\right]\end{array}\right)$$

$$\xrightarrow[\text{replaced by}]{}\sigma^2_{mn}\left[\cos(c_{mn,i})\times\cos(c_{mn,j})+\sin(c_{mn,i})\times\sin(c_{mn,j})\right] \tag{21}$$

Once the covariances $\{C_{ij}\}$ are calculated, the variance of the curve average can be easily derived. Let the lengths of the n line segments be denoted by (L_1, L_2, …, L_n). The curve average, denoted by W_C, can then be approximated as the weighted sum of (W_{S1}, W_{S2}, …, W_{Sn}):

$$W_C \approx \frac{1}{L}\sum_{i=1}^{n} L_i\, W_{Si} \tag{22}$$

where $L = L_1 + \ldots + L_n$ is the sum of all lengths; W_{Si} is the line average along the i-th line segment. W_C is therefore a normal random variable with mean = 0 and variance equal to

$$\sigma_C^2 = Var(W_C) \approx \frac{1}{L^2}\sum_{i=1}^{n}\sum_{j=1}^{n} C_{ij}\, L_i\, L_j \tag{23}$$

where C_{ij} can be evaluated by Eqs. (18) ~ (21). The variance reduction factor for the averaging effect along the curve is equal to

$$\Gamma_C^2 = \sigma_C^2 / \sigma^2 \approx \frac{1}{L^2\sigma^2}\sum_{i=1}^{n}\sum_{j=1}^{n} C_{ij}\, L_i\, L_j \tag{24}$$

Finally, the (approximate) curve average W_C can be directly simulated by the following equation:

$$W_C = \sqrt{\Gamma_C^2}\cdot\sigma\cdot Z \tag{25}$$

where Z is a standard normal random variable. It is not necessary to first simulate the point process $W(x, z)$ and do the integration along the curve.

3.1 Validation of the Proposed C_{ij} Equation

Equation (18) is central to this study. It computes the covariance between W_{Si} and W_{Sj} (W_{Si} and W_{Sj} are the line averages along S_i and S_j in 2D). In this subsection, Eq. (18) is compared to the analytical solutions in 1D, namely Eq. (12). This is done by letting $\delta_x = \infty$ so that a 2D random field reduces to 1D. Let (S_i, S_j) be two line segments with lengths (L_i, L_j). The comparison is conducted in two scenarios: (A) S_i and S_j have the same length ($L_i = L_j = 10$) but different end points ($z_{0,i} \neq z_{0,j}$) (see Fig. 5(a)); (B) S_i and S_j share the same end point ($z_{0,i} = z_{0,j} = 0$) but have different lengths ($L_i \neq L_j$) (see Fig. 5(b)). $\sigma = 1$ and $\delta_z = 1$ are adopted for both scenarios. The comparison results for scenarios A and B are shown in Figs. 6 and 7, respectively, where the computed C_{ij} is normalized by the standard deviations of W_{Si} and W_{Sj} (*i.e.*, the correlation coefficient is compared). The analytical solutions based on Eq. (12) are plotted as solid lines, whereas the results based on Eq. (18) are plotted as dashed lines. Figures 6 and 7 show that Eqs. (12) and (18) give nearly identical results (solid and dashed lines nearly coincide) for both the SExp and QExp models.

3.2 Validation of the Variance Reduction Γ^2_C

Equation (24) computes the approximate variance reduction factor for the curve averaging in 2D. In this subsection, the results based on Eq. (24) are compared to the 1D analytical solutions based on Eq. (14). This is done by considering a special case of a 2D curve: A straight line in 2D. The curve averaging along this curve (a straight line in 2D) reduces to a 1D line averaging so that Eq. (14) can be used to compute the 1D analytical solutions. The comparison is conducted in three scenarios: (A) the curve is a horizontal straight line (x-direction) with total length $L = 10$; (B) the curve is a vertical straight line (z-direction) with total length $L = 10$; (C) the curve is a 45° straight line with total length $L = 10$. The squared exponential (QExp) model is adopted, and $\sigma = 1$, $\delta_x = 20$ and $\delta_z = 1$ are adopted for all scenarios. The 1D analytical solutions for the variance reduction factors can be computed using Eq. (14) with $D = 10$ and δ = SOF along the line direction, which are 20, 1, and 1.412, respectively. The resulting analytical solutions for $\Gamma^2(D)$ are shown in Table 1. Equation (24) is also used to compute the variance reduction factor Γ^2_C due to curve averaging. The number of line segments is taken to be $n = 1$, 4, 16, and 64. Taking Scenario (C) with $n = 4$ as an example, the following matrix is the covariance matrix produced by Eq. (18):

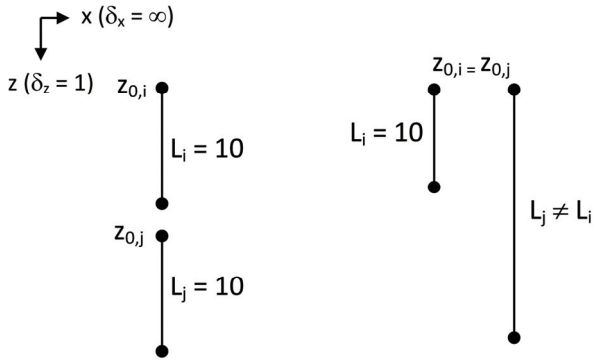

(a) Scenario A (b) Scenario B

Fig. 5 Two scenarios of S_i and S_j

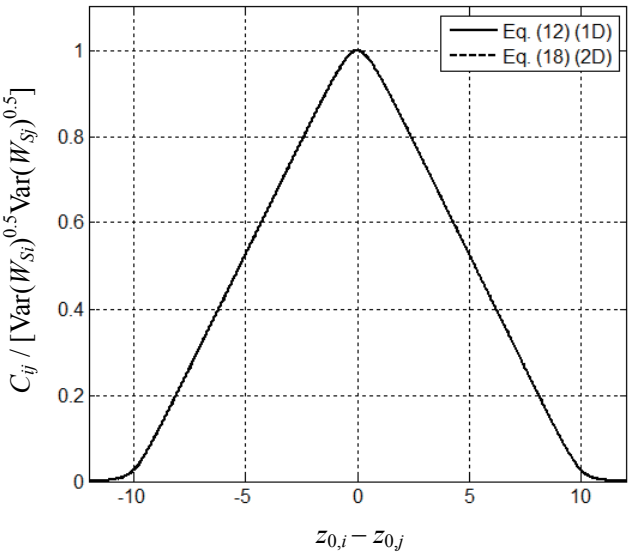

(a) SExp model

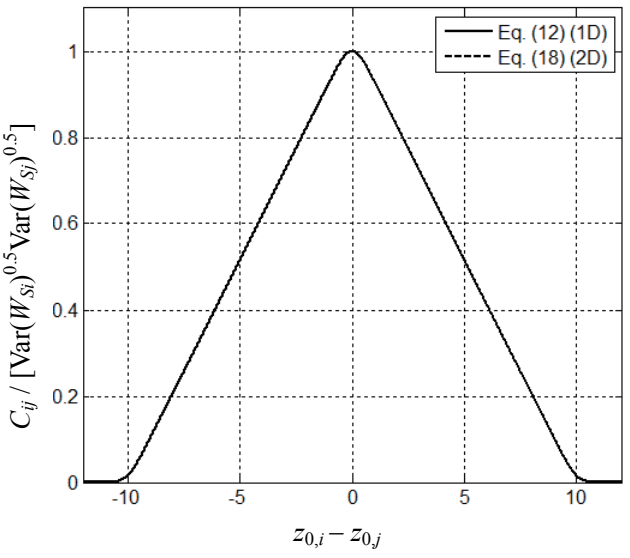

(b) QExp model

Fig. 6 The comparison results for the computed C_{ij} (Scenario A)

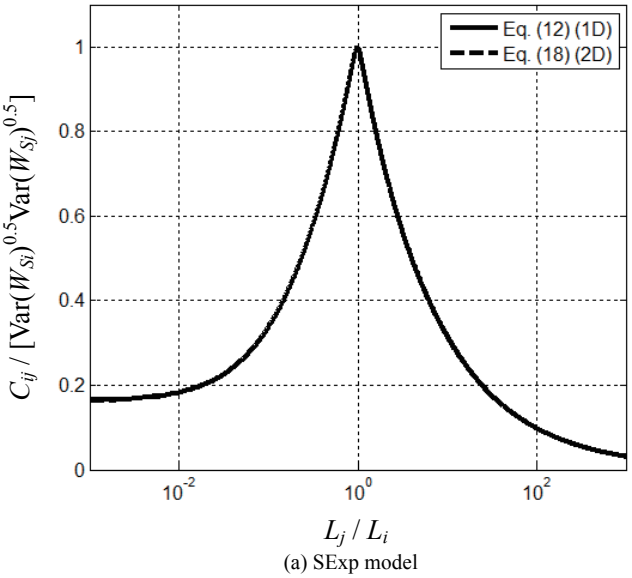

(a) SExp model

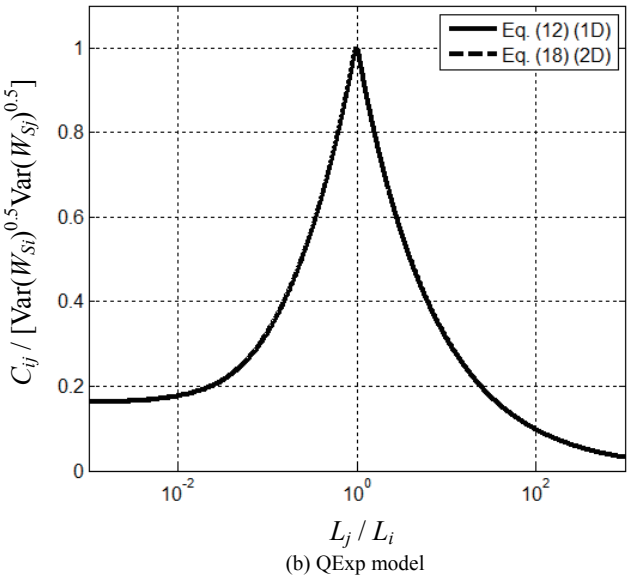

(b) QExp model

Fig. 7 The comparison results for the computed C_{ij} (Scenario B)

$$\mathbf{C} = \begin{bmatrix} C_{11} & C_{12} & C_{13} & C_{14} \\ & C_{22} & C_{23} & C_{24} \\ & & C_{33} & C_{34} \\ SYM. & & & C_{44} \end{bmatrix} = \begin{bmatrix} 0.4634 & 0.0508 & 0 & 0 \\ & 0.4634 & 0.0508 & 0 \\ & & 0.4634 & 0.0508 \\ SYM. & & & 0.4634 \end{bmatrix} \quad (26)$$

Γ^2_C is therefore computed using Eq. (24), which gives Γ^2_C = 0.1349. Table 1 shows the computed variance reduction factors using Eqs. (14) and (24). It is clear that they give nearly identical results. Moreover, the variance reduction factors due to curve averaging are independent of n = 1, 4, 16, or 64. Some other scenarios with different (δ_x, δ_z) or with the SExp model are also validated, although not shown here.

Table 1 The computed variance reduction factors using Eqs. (14) and (24)

Scenario	SOF along the line segment (δ)	Length of the line segment (D)	1D analytical solution for Γ^2 [Eq. (14)]	Γ^2 computed by Eq. (24)			
				n = 1	n = 4	n = 16	n = 64
(A) x-direction	20	10	0.8871	0.8871	0.8871	0.8871	0.8871
(B) z-direction	1	10	0.0968	0.0968	0.0968	0.0968	0.0968
(C) incline at 45°	1.412	10	0.1349	0.1349	0.1349	0.1349	0.1349

4. EXAMPLES OF APPLICATIONS

4.1 Averaging Effect over the Shaft Area of a Pile

A 12 m long pile with a diameter B = 0.8 m is to be installed in a deposit of clay. From the results of field and laboratory tests on the clay, the undrained shear strength (s_u) has mean value = 40 kN/m^2, coefficient of variation (COV) = 0.4, $\delta_x = \delta_y$ = 50 m, and δ_z = 2 m (x and y are the two horizontal directions; z is the depth direction). The ACF is the SExp model. This example is extracted from Orr (2014) but slightly modified. The goal is to compute the COV of the averaged s_u value over the entire pile shaft area. Note that the mean of the averaged s_u remains 40 kN/m^2. The variance reduction factor over the entire shaft area (Γ^2_{shaft}) takes the following form:

$$\Gamma^2_{shaft} = \Gamma^2_{circle} \times \Gamma^2_z \quad (27)$$

where Γ^2_{circle} is the variance reduction factor for the curve averaging over the circle, whereas Γ^2_z is the variance reduction factor for the line averaging over the depth. The circle is approximated by n line segments, as shown in Fig. 8. Γ^2_z can be computed analytically using Eq. (14) with D = 12 m and $\delta = \delta_z$ = 2 m (SExp model):

$$\Gamma^2_z = \left[2\times 12/2 - 1 + \exp(-2\times 12/2)\right] \Big/ (2\times 12^2/2^2) = 0.1528 \quad (28)$$

Averaging Effect over the Circle

Equation (24) is used to approximately compute Γ^2_{circle}. n should be sufficiently large for the curve representation to be accurate. Figure 9 shows how Γ^2_{circle} changes with B/δ for various choices of n for scenarios with $\delta_x = \delta_y = \delta$. In this figure, B/δ ranges from 0.001 to 100. This sufficiently covers the practical range of interest for pile designs. By inspecting Fig. 9, $n \geq 20$ is sufficient, because a larger n does not produce a noticeably more accurate result. In the following, only the results with n = 40 will be presented.

Figure 10(a) shows how Γ^2_{circle} changes with B/δ_y for more general cases with $\delta_x \neq \delta_y$. Γ^2_{circle} is approximately computed by Eq. (24) (SExp model). Several δ_x/δ_y ratios are considered (δ_x/δ_y = 1, 2, 5, 10, 100). The current case is with δ_x/δ_y = 1 and B/δ_y = 0.8/50 = 0.016. By checking Fig. 10(a), Γ^2_{circle} is approximately 0.9745. Note that this is nearly the exact value for Γ^2_{circle},

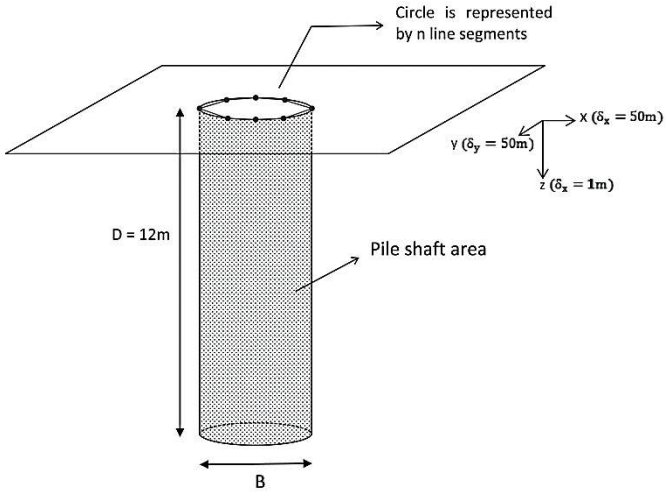

Fig. 8 The schematic of the pile

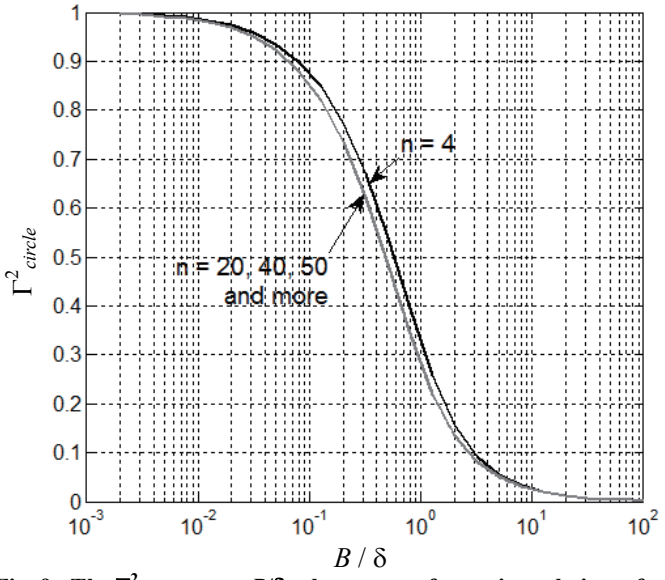

Fig. 9 The Γ^2_{circle} versus B/δ relationships for various choices of n

not a rough approximation, because Eq. (24) is nearly exact with $n = 40$. The overall variance reduction factor $\Gamma^2_{shaft} = \Gamma^2_{circle} \times \Gamma^2_z = 0.1489$. This means that the COV of the averaged s_u value over the entire pile shaft area is equal to $0.4 \times (0.1489)^{0.5} = 0.154$.

Γ^2_{circle} can be also estimated using a simplified method proposed by El-Ramly *et al*. (2006). They proposed the following equivalent isotropic SOF:

$$\delta_E = \sqrt{\delta_x \cdot \delta_y} \tag{29}$$

For the current case, $\delta_E = (\delta_x \delta_y)^{0.5} = 50$ m. Then, Γ^2_{circle} can be approximately estimated using Eq. (14) with $D = \pi B = 2.51$ m and $\delta = \delta_E = 50$ m. Hence, $\Gamma^2_{circle} = 0.9673$, and the overall variance reduction factor $\Gamma^2_{shaft} = \Gamma^2_{circle} \times \Gamma^2_z = 0.1478$, which is slightly smaller than the result given by Eq. (24). In Fig. 10(b), the results estimated by El-Ramly *et al*.'s simplified method are also plotted for comparison. For the cases with $\delta_x/\delta_y \le 2$, this simplified method is quite accurate, producing results that are

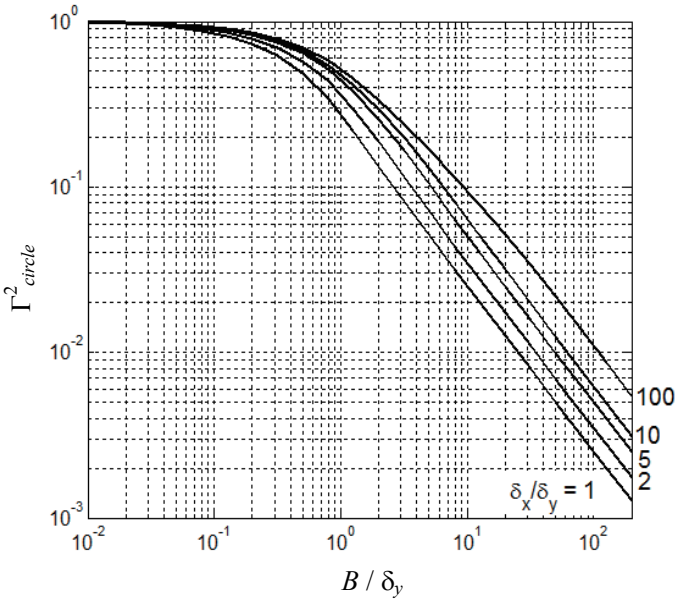

(a) Γ^2_{circle} computed by Eq. (24)

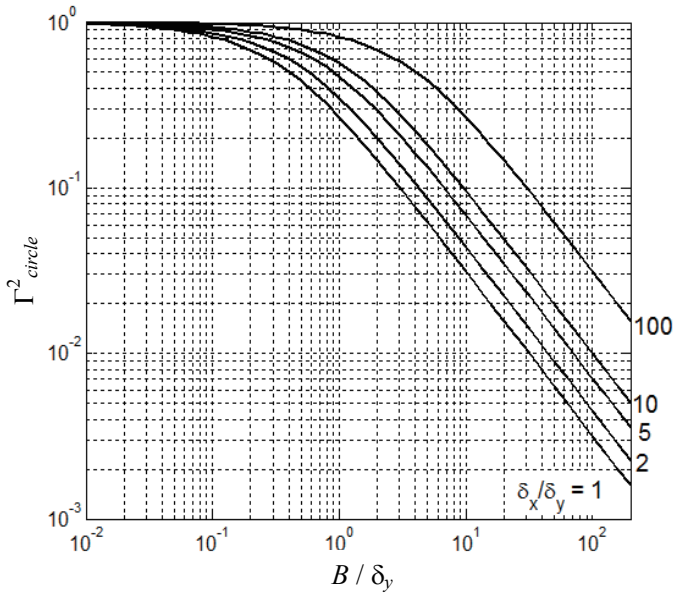

(b) Γ^2_{circle} computed by equivalent isotropic δ_E

Fig. 10 The Γ^2_{circle} versus B/δ_y relationships for various choices of δ_x/δ_y ratios (SExp model)

fairly close to the results computed by Eq. (24). However, for the cases with $\delta_x/\delta_y \ge 5$, this simplified method always overestimates the variance reduction factor (*i.e.*, conservative). The overestimation is quite severe (*i.e.*, overly conservative) for the case with $\delta_x/\delta_y = 100$. Figure 11 further plots the Γ^2_{circle} versus B/δ_y relationships for the QExp model. The conclusion is similar, except that for the cases with $\delta_x/\delta_y \le 2$, the simplified method proposed by El- Ramly *et al*. (2006) is not as accurate as in the SExp cases.

4.2 Reliability of a Circular Trial Slip Curve in 2D Slope Stability

Consider a circular trial slip curve in an undrained slope, as shown in Fig. 2. There are three clay layers in this slope. The s_u

for each layer is modeled as a stationary normal random field. The statistical properties of the three random fields are shown in Table 2. The three random fields are assumed mutually independent. The unit weights for the three clay layers are all equal to 20 kN/m^3. The trial slip curve is divided into 9 line segments (S_1, …, S_9), which are the bases of the 9 slices. Table 3 shows the information for all slices and line segments. The coordinates for the two end points of each line segment, namely ($x_{0,i}$, $z_{0,i}$) and ($x_{1,i}$, $z_{1,i}$), are also listed in Table 3. The overall factor of safety (FS) can be computed using the Swedish circle ($\phi = 0$) method (Fellenius 1922; Duncan and Wright 2005):

$$FS = \frac{\text{resisting moment due to soil shear resistance}}{\text{overturning moment due to soil self weight}} = \frac{r \times L \times \overline{s}_u}{\sum_{i=4}^{9} b_i W_i - \sum_{i=1}^{3} b_i W_i} \tag{30}$$

where r = 30 m is the radius of the trial circle; L = 45.33 m is the total length of the circular curve; $\overline{s}_u$ is the average along the circular trial slip curve (curve average); W_i is the total weight of the i-th slice, and b_i is its moment arm. Table 3 shows the information for (W_i, b_i). Note that the first three slices contribute to the resisting moment.

Table 2 The statistical properties of the s_u random fields

Clay layer	Mean value μ (kN/m^2)	Standard deviation (kN/m^2)	COV	Horizontal SOF δ_x (m)	Vertical SOF δ_z (m)
1	20	(0, 0)	0.3	30	1
2	30	(3.80, –1.80)	0.2	30	2
3	50	(7.6, –3)	0.3	30	2

Table 3 The information for each slice and slice base

Index (i)	Length of the i-th slice base (or the i-th line segment) (L_i) (m)	Left-hand-side end point ($x_{0,i}$, $z_{0,i}$) (m)	Right-hand-side end point ($x_{1,i}$, $z_{1,i}$) (m)	Weight of the i-th slice (W_i) (kN/m)	Moment arm (b_i) (m)
1	4.20	(0, 0)	(3.80, –1.80)	68.38	12.18
2	3.98	(3.80, –1.80)	(7.6, –3)	182.34	8.86
3	4.81	(7.6, –3)	(12.34, –3.76)	443.41	4.47
4	4.74	(12.34, –3.76)	(17.09, –3.76)	694.70	0.13
5	4.81	(17.09, –3.76)	(21.83, –3)	883.63	4.81
6	4.98	(21.83, –3)	(26.55, –1.42)	992.37	9.51
7	5.37	(26.55, –1.42)	(31.27, 1.13)	933.58	14.12
8	6.11	(31.27, 1.13)	(36, 5)	654.99	18.70
9	6.41	(36, 5)	(40, 10)	200.17	22.62

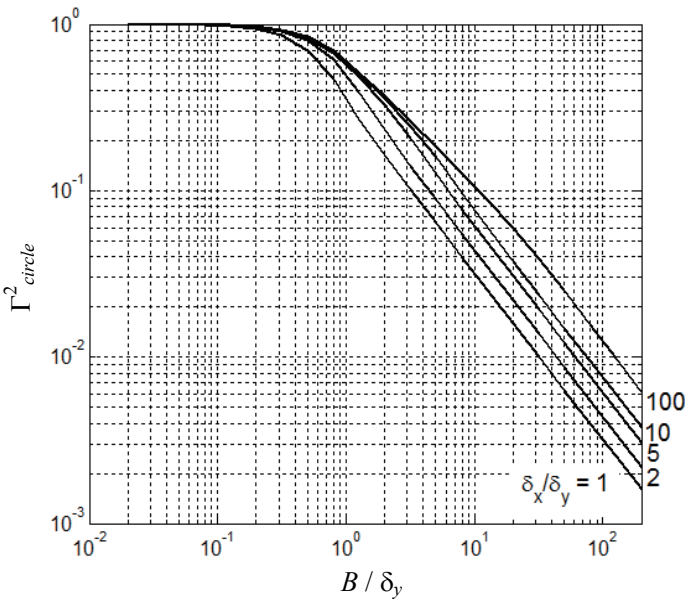

(a) Γ^2_{circle} computed by Eq. (24)

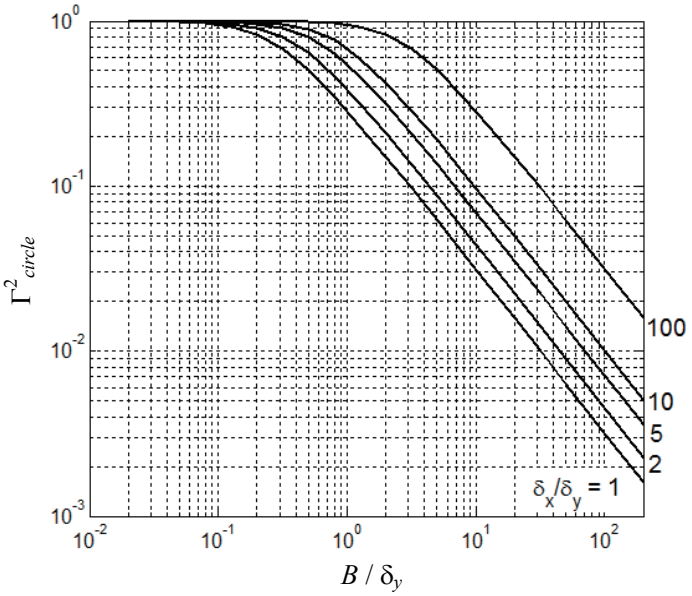

(b) Γ^2_{circle} computed by equivalent isotropic δ_E

Fig. 11 The Γ^2_{circle} versus B/δ_y relationships for various choices of δ_x/δ_y ratios (QExp model)

The mean value of $\overline{s}_u$ is approximately equal to (see Eq. (22))

$$E(\overline{s}_u) \approx \frac{1}{L}\sum_{i=1}^{9} L_i \, \mu_i \tag{31}$$

where L_i is the length of the i-th line segment (see Table 3); μ_i is the s_u mean value for the clay layer underlying the i-th slice. The resulting mean value of $\overline{s}_u$ is 34.92 kN/m^2. Using Eq. (18), the covariance matrix for the 9 line averages can be constructed:

$$\mathbf{C} = \begin{bmatrix} 20.18 & 8.06 & 0 & 0 & 0 & 2.73 & 2.83 & 0.17 & 0 \\ 8.06 & 23.42 & 0 & 0 & 0 & 6.86 & 1.15 & 0.05 & 0 \\ 0 & 0 & 161.93 & 118.01 & 95.02 & 0 & 0 & 0 & 0 \\ 0 & 0 & 118.01 & 202.77 & 118.01 & 0 & 0 & 0 & 0 \\ 0 & 0 & 95.02 & 118.01 & 161.93 & 0 & 0 & 0 & 0 \\ 2.73 & 6.86 & 0 & 0 & 0 & 20.97 & 5.32 & 0.22 & 0 \\ 2.83 & 1.15 & 0 & 0 & 0 & 5.32 & 16.86 & 2.79 & 0 \\ 0.17 & 0.05 & 0 & 0 & 0 & 0.22 & 2.79 & 13.15 & 0 \\ 0 & 0 & 0 & 0 & 0 & 0 & 0 & 0 & 6.33 \end{bmatrix} \quad (32)$$

Note that there are lots of zeros in the covariance matrix because the three s_u random fields are independent. The line segments (S_1, S_2) lie in the same clay layer as (S_6, S_7, S_8). Hence, the corresponding off-diagonal entries are non-zero. The variance of $\overline{s}_u$ can be determined using Eq. (23): $\sigma^2_C \approx 15.04$ (kN/m^2)^2. Note that this result is nearly exact. This means that $\overline{s}_u$ is a normal random variable with mean = 34.92 kN/m^2 and standard deviation = 3.88 kN/m^2. The failure probability is equal to the probability for $FS < 1$, which is estimated to be 0.0604 (using Monte Carlo simulation with sample size = 10^6).

5. CONCLUSIONS

This study proposes a new method of simulating a curve average in a two-dimensional (2D) stationary normal random field. The proposed method is based on the Fourier series method developed by Jha and Ching (2013). With the help of the Fourier series, the covariance between any two 2D line segments has an analytical expression. Because a curve can be represented as a series of connecting line segments, it is possible to derive the analytical expression for the variance reduction factor due to the averaging along the curve. Therefore, the curve average can be readily simulated. The accuracy of the proposed method is examined by comparing its results to chosen 1D examples with analytical solutions. The examination shows that the proposed method produces results that are nearly identical to the analytical solutions.

Two examples are used to demonstrate the applications of the proposed method. It is shown that the simplified method of calculating the variance reduction factor proposed by El-Ramly *et al*. (2006) is fairly effective for the cases with weak spatial anisotropy (horizontal and vertical SOFs are not significantly different). However, for the cases with strong spatial anisotropy (horizontal SOF is significantly larger than the vertical SOF), the simplified method generally overestimates the variance reduction factor for the curve averaging.

The MATLAB codes for simulating the curve average and computing the variance reduction factor are available to the readers upon request (please contact the first author).

REFERENCES

Asaoka, A. and Grivas, D. A. (1982). "Spatial variability of the undrained strength of clays." *Journal of Geotechnical Engineering*, ASCE, **108**(5), 743–756.

Cao, Z., Wang, J., and Wang, Y. (2013). "Effects of spatial variability on reliability-based design of drilled shafts." *Foundation Engineering in the Face of Uncertainty: Honoring Fred H. Kulhawy*, ASCE GSP 229, 602–616.

Ching, J. and Liao, H.-J. (2013). "Re-analysis of Freeway-3 dip slope failure case—A spatial variability view." *Journal of GeoEngineering*, **8**(1), 1–10.

Ching, J. and Phoon, K. K. (2013a). "Mobilized shear strength of spatially variable soils under simple stress states." *Structural Safety*, **41**, 20–28.

Ching, J. and Phoon, K. K. (2013b). "Probability distribution for mobilized shear strengths of spatially variable soils under uniform stress states." *Georisk*, **7**(3), 209–224.

Cho, S. E. (2007). "Effects of spatial variability of soil properties on slope stability." *Engineering Geology*, **92**, 97–109.

Chok, Y. H., Jaksa, M. B., Griffiths, D. V., Fenton, G. A., and Kaggwa, W. S. (2007). "A parametric study on reliability of spatially random cohesive soils." *Australian Geomechanics*, **42**(2), 7985.

Duncan, J. M. and Wright, S. G. (2005). *Soil Strength and Slope Stability*. John Wiley and Sons, New Jersey, USA.

El-Ramly, H., Morgenstern, N. R., and Cruden, D. M. (2002). "Probabilistic slope stability analysis for practice." *Canadian Geotechnical Journal*, **39**, 665–683.

El-Ramly, H., Morgenstern, N. R., and Cruden, D. M. (2006). "Lodalen slide: A probabilistic assessment." *Canadian Geotechnical Journal*, **43**, 956–968.

Fellenius, W. (1922). *Statens Jarnjvagars Geoteknniska Commission*. Stockholm, Sweden.

Fenton, G. A. and Vanmarcke, E. H. (1990). "Simulation of random fields via local average subdivision." *Journal of Engineering Mechanics*, ASCE, **116**(8), 1733–1749.

Fenton, G. A. and Griffiths, D. V. (2003). "Bearing capacity prediction of spatially random *c*-φ soils." *Canadian Geotechnical Journal*, **40**(1), 54–65.

Griffiths, D. V. and Fenton, G. A. (2004). "Probabilistic slope stability analysis by finite elements." *Journal of Geotechnical and Geoenvironmental Engineering*, ASCE, **130**(5), 507–518.

Griffiths, D. V., Huang, J., and Fenton, G. A. (2010). "Probabilistic infinite slope analysis." *Computers and Geotechnics*, **38**(4), 577–584.

Jha, S. K. and Ching, J. (2013). "Simulating spatial averages of stationary random field using Fourier series method." *Journal of Engineering Mechanics*, ASCE, **139**(5), 594–605.

Nishimura, S., Murakami, A., and Matsuura, K. (2010). "Reliability-based design of earth-fill dams based on the spatial distribution of strength parameters." *Georisk*, **4**(3), 140–147.

Orr, T. L. L. (2014). "Managing risk and achieving reliable geotechnical designs using Eurocode 7." *Risk and Reliability in Geotechnical Engineering*, Eds., K.K. Phoon & J. Ching, Taylor & Francis (in press).

Phoon, K. K., Quek, S. T., and An, P. (2003). "Identification of statistically homogeneous soil layers using modified Bartlett statistics." *Journal of Geotechnical and Geoenvironmental Engineering*, ASCE, **129**(7), 649–659.

Soulie, M., Montes, P., and Silvestri, V. (1990). "Modelling spatial variability of soil parameters." *Canadian Geotechnical Journal*, **27**(5), 617–630.

Vanmarcke, E. H. (1977). "Probabilistic modeling of soil profiles." *Journal of Geotechnical Engineering*, ASCE, **103**(11), 1227–1246.

Vanmarcke, E. H. (1983). *Random Fields: Analysis and Synthesis*. The MIT Press, Cambridge, Massachusetts.

Wang, Y., Cao, Z., and Au, S. K. (2011). "Practical reliability analysis of slope stability by advanced Monte Carlo simulations in a spreadsheet." *Canadian Geotechnical Journal*, **48**(1), 162–172.